Metabolomic variability of four macroalgal species of the genus Lobophora using diverse approaches

Julie Gaubert, Stephane Greff, Olivier P. Thomas, Claude Payri

Metabolomic variability of four macroalgal species of the genus *Lobophora* using diverse approaches

Julie Gaubert[a,b], Stéphane Greff[c], Olivier P. Thomas[d,**], Claude E. Payri[b,*]

[a] Sorbonne Universités, Collège Doctoral, F-75005 Paris, France

[b] UMR ENTROPIE (IRD, UR, CNRS), Institut de Recherche pour le Développement, B.P. A5, 98848 Nouméa Cedex, Nouvelle-Calédonie, France

[c] Institut Méditerranéen de Biodiversité et d'Ecologie Marine et Continentale (IMBE), UMR 7263 CNRS, IRD, Aix Marseille Université, Avignon Université, Station Marine d'Endoume, rue de la Batterie des Lions, 13007 Marseille, France

[d] Marine Biodiscovery, School of Chemistry and Ryan Institute, National University of Ireland Galway (NUI Galway), University Road, H91 TK33 Galway, Ireland

Abstract

Among comparative metabolomic studies used in marine sciences, only few of them are dedicated to macroalgae despite their ecological importance in marine ecosystems. Therefore, experimental data are needed to assess the scopes and limitations of different metabolomic techniques applied to macroalgal models. Species of the genus *Lobophora* belong to marine brown algae (Family: Dictyotaceae) and are widely distributed, especially in tropical coral reefs. The species richness of this genus has only been unveiled recently and it includes species of diverse morphologies and habitats, with some species interacting with corals. This study aims to assess the potential of different metabolomic fingerprinting approaches in the discrimination of four well known *Lobophora* species (*L. rosacea, L. sonderii, L. obscura* and *L. monticola*). These species present distinct morphologies and are found in various habitats in the New Caledonian lagoon (South-Western Pacific).We compared and combined different untargeted metabolomic techniques: liquid chromatography-mass spectrometry (LC-MS), nuclear magnetic resonance (^{1}H-NMR) and gas chromatography (GC-MS). Metabolomic separations were observed between each *Lobophora* species, with significant differences according to the techniques used. LC-MS was the best approach for metabotype distinction but a combination of approaches was also useful and allowed identification of chemomarkers for some species. These comparisons provide important data on the use of metabolomic approaches in the *Lobophora* genus and will pave the way for further studies on the sources of metabolomic variations for this ecologically important macroalgae.

Keywords: *Lobophora* – Dictyotaceae – macroalgae – metabolomic – fingerprinting – comparative approach – New Caledonia

1.Introduction

Specialized metabolites are often considered as low molecular weight molecules, end products of cellular regulatory processes, and final responses of biological systems to genetic and/or environmental changes (Fiehn, 2002). They can be regarded as products of natural selection during evolution. These secondary metabolites play also an important role in shaping algal chemical diversity (Wink, 2003). The set of metabolites present in the organisms can be highly complex and their biosynthesis can also be related to the associated microbiota (Roessner and Bowne, 2009). Traditionally, the chemical composition of an organism is explored through natural product chemistry which includes long and tedious steps of isolation and structure elucidation of metabolites (Robinette et al., 2011). This approach is time consuming and incomplete as it focuses mostly on the major compounds produced. Recent advances in more global approaches called metabolomics allow the analysis of a wider part of the metabolome by the simultaneous detection of hundreds to thousands of the metabolites of a small sample in a short period of time. In environmental sciences, metabolomics has therefore appeared as a quick and useful approach to examine the metabolite diversity of species and study their variations with time, geography, biotic interactions or other environmental factors (Bundy et al., 2009). Compared to the plant kingdom, relatively few environmental metabolomics studies have been reported on marine organisms. Taxonomy-based metabolomics has been applied for marine organisms like sponges (Ivanišević et al., 2011a; Pérez et al., 2011), zoanthids (Costa-Lotufo et al., 2018; Jaramillo et al., 2018) and microalgae (Mooney et al., 2007). Variability in the metabolomic profiles were explored in time and space for some sponges (Rohde et al., 2012), ascidians (López-Legentil et al., 2006), zoanthids (Cachet et al., 2015) and corals (Slattery et al., 2001) but also in response to environmental factors like temperature or salinity (Abdo et al., 2007; Bussell et al., 2008).

Among the chemical studies dedicated to macroalgae, only a few used metabolites as a taxonomic tool targeting specific compounds or classes like phenolics (Connan et al., 2004) or diterpenes (Campos De Paula et al., 2007). While these studies traditionally focus on potentially active compounds with pharmaceutical interests, a more global approach using metabolomics can represent a useful tool to explore the metabolome of macroalgae and its fluctuations. For example, metabolomics was applied on the red alga *Asparagopsis taxiformis* to study the spatio-temporal variation of its metabolome (Greff et al., 2017). Another study on the red alga *Portieria hornemannii* explored different sources for the variation of non-polar metabolites between cryptic species and life stages (Payo et al.,2011). Metabolomics also appeared as a complementary tool to understand defense or tolerance mechanisms of macroalgae in an ecological context (Rempt et al., 2012; Ritter et al., 2014). Marine brown macroalgae from the genus *Lobophora* (Family Dictyotaceae) have already been studied chemically. Gerwick & Fenical (1982) first described 1-(2,4,6-trihydroxyphenyl)hexadecan-1-one in *L. papenfussii.* Three sulfoquinovosyldiacylglycerols (SQDGs) and later lobophorolide were identified from *L. variegate* (Cantillo-Ciau et al., 2010; Kubanek et al., 2003). Recently, seven nonadecaketides named lobophorols, lobophopyranones and lobophorones (Gutiérrez-Cepeda et al., 2015) were found in the Atlantic *L. variegate* while the polyunsaturated lobophorenols A, B and C were described in the tropical *L. rosacea* (Vieira et al., 2016). Abundant in tropical coral reef habitats, some *Lobophora* species are closely associated with corals and therefore strongly involved in coral-algal interactions (Rasher & Hay, 2010), leading in some cases to negative impacts on corals. The high specific diversity of *Lobophora* genus has recently been unveiled (Vieira et al.,2014, 2017), with species exhibiting various morphologies and habitats, questioning the link between chemical diversity and

species diversity. Due to this chemical diversity, species of this genus are therefore good candidates to undergo metabolomics-based study to explore the metabolic variability among the different species.

We first decided to assess the potential of different approaches in metabolomic fingerprinting to separate four well-known *Lobophora* species (*L. rosacea, L. sonderii, L. obscura* and *L. monticola*), with distinct morphology and present in diverse habitats of the New Caledonian lagoon (South-Western Pacific). The systematics of these species being well described, we aimed at providing important insights on the relevance of these approaches to first discriminate species. The results of these preliminary data will then pave the way for deeper metabolomic studies on the presence of cryptic species, the influence of environmental parameters or biotic factors like the reproductive cycles. In terms of reproduction, little is known about *Lobophora* in New Caledonia and this genus is supposed to be reproductive all year round (Vieira, pers. com.). Our knowledge on the main specialized metabolites found in *L. rosacea* was a prerequisite to guide our study as they are presumed to have a taxonomic relevance. We used untargeted metabolomic approaches using three different techniques: UHPLC-MS-QToF, ^{1}H-NMR and GC-MS followed by unsupervised and supervised analyses to highlight chemical differences among species.

2.Results

2.1.^{1}H-NMR

The matrix obtained after data analyses was composed of 7,998 buckets. A value of 33.5% of variance was explained by the two first components of the PCA (Fig. 1a) and mainly due to *L. rosacea* characterized by a different metabolomic fingerprint than the other three species (PPLS-DA, CER = 0.328, $p = 0.001$, post hoc $p < 0.05$, Fig. 1b,Table S1**).** In the central cluster of the PCA that grouped the three other species, only *L. monticola* and *L. obscura* present significant different metabolomic fingerprints ($p = 0.018$), whereas *L. sonderii* is not chemically different from the two others (Table S1, $p > 0.05$).

The overlay of ^{1}H NMR spectra (Fig. 2), indicated that the major signals are shared by all *Lobophora* species: intense signals at δ_H 1-2 ppm due to the methylenes of long chain fatty acids, and signals at δ_H 2.8 and 5.3 ppm attributed to carbon-carbon unsaturations. More variable regions containing characteristic signals of the polyunsaturated lobophorenols A, B and C were observed between δ_H 3.2-4.5 (chlorinated and hydroxylated methines), 4.8-5.2 and 5.0-5.8 ppm (terminal olefinic protons, Fig. 2 and S1). Due to the high number of generated bins, Kruskal-Wallis loading plot (Fig. S2) was used to identify chemical markers, which separate metabolic diversity of *Lobophora* species (with $p < 0.05$, Table S2). The regions corresponding to the signals of lobophorenols are the main markers of differences between species and are mostly present in *L. rosacea.*

2.2.UHPLC-QToF

After LC-MS data analyses and filtering, 600 metabolic features were finally considered. The variance on the two first components of the PCA was explained by 38.7% (Fig.1c), a value slightly higher than for NMR analysis. The LC-MS approach permitted a better separation of each species' metabolome than NMR (CER =

0.115, p = 0.001, p< 0.05 for each tested pair, Fig. 1d, Table S1). The difference between chemical groups was mainly quantitative as shown in the Venn diagram (Fig. S4).

Among chemomarkers, two compounds, lobophorenol B (*m/z* 334.272 $[M + NH_4]^+$, $C_{21}H_{32}O_2$) and lobophorenol C (*m/z* 336.287 $[M + NH_4]^+$, $C_{21}H_{34}O_2$), previously isolated in *L. rosacea* (Vieira et al., 2016) were mainly detected in this species (Fig. 3, Table S3). They were also detected in *L. monticola*, but with high variability and not in *L. sonderii* and *L. obscura*. The other chemomarkers of each species were tentatively annotated based on the construction of a molecular network but no other match was found in the current database, with the majority of them appearing as minor intensity ions.

To combine data obtained by LC-MS with those by NMR, a multiple factor analysis (MFA) was performed (Fig. 4). The four *Lobophora* species were well separated despite a lower variance of 21.7% on the two first dimensions.

2.3. GC-MS

The richness in non-polar specialized metabolites in *Lobophora* led us to analyze the CH_2Cl_2 fractions by GC-MS while attempts to use NMR for those fractions were unfruitful due to intense lipidic peaks. The explained variance on axis 1-2 of the PCA was 35.7%, a value similar to the values obtained with the two other techniques (Fig.1e). All algal metabotypes were differentiated with this technique (CER = 0.304, p = 0.001, Fig.1f) except for *L. monticola* vs *L. rosacea* (p = 0.431, Table S1). Among the chemomarkers contributing to the discrimination of the species metabotypes, we identified a small carboxylic acid: 2-pentenoic acid (M5), an amide: maleimide, 2-methyl-3-vinyl (M18), and two esters: methyl stearate (M38) and hexanoic acid, 2-ethyl-, hexadecyl ester (M48) (Table 1). M5 and M48 are specific to *L. obscura* while this species contained lower amount of M38 compared to the three other species. *Lobophora sonderii* and *L. rosacea* exhibit higher levels of M18 (Fig. S5).

Moreover, some compounds known as plastic pollutants were found in all species and contribute to differences in their chemical profiles (Phenol, 2,4-di-*tert*-butyl; tributyl acetyl citrate; *o*-xylene; naphthalene, 2,6-dimethyl-; *p*-cresol, 2,6-di-*tert*-butyl-; *N*-methyl-*N*-benzyltetradecanamine).

3. Discussion

Even though LC-MS is a method largely employed in metabolomics studies due to its high sensitivity, it is not suitable for all metabolites and more appropriate for polar, weakly polar and neutral compounds (Wang et al., 2015). Moreover, it relies on ionization process, limiting the study of poorly-ionizable compounds. GC-MS is then more suitable when non-polar metabolites are found as the main major specialized metabolites. On the contrary and even if much less sensitive, NMR is more universal and does not rely on ionization processes nor the separation of analytes by HPLC, and solubilization of the metabolites is the only limitation. NMR spectra are able to provide a better snapshot of what are the major metabolites and their relative concentrations in the studied specimens. This information is highly relevant for major metabolites that may correspond to specialized

metabolites providing useful information concerning species discrimination. NMR would therefore be less affected by environmental changes often linked to minor metabolites (Ivanišević et al., 2011b).

The four species of *Lobophora* are well described morphologically and their phylogeny resolved in 2014 using mitochondrial gene Cox3 (Vieira et al., 2014). *Lobophora monticola*, *L. obscura*, *L. rosacea* and *L. sonderii* are distantly-related species. They are distributed evenly across the *Lobophora* evolutionary tree, with *L. rosacea* the most basal species of the four (Fig. S6)(Vieira et al., 2014, 2017). In the current study, the algal species have been separated based on their metabolomic fingerprints, and depending on the used technique. The LC-MS approach was the most effective technique for the separation of the four species of this genus (PPLS-DA, CER = 0.115), but NMR and GC-MS (CER_{NMR} = 0.328, $CER_{GC/MS}$ = 0.304) also provided interesting complementary results. While less sensitive than LC-MS or GC-MS, NMR provides the highest reproducibility among metabolomic measuring platforms (Farag et al., 2012a).

In our study, NMR analyses performed on the same methanolic fractions as LC-MS allowed a clear distinction of *L. rosacea* from the other three species, in agreement with phylogenetic data where this species appears as the most basal. Like LC-MS, NMR highlighted lobophorenols as discriminating metabolites in *L. rosacea*, with most of the signals responsible for the chemical divergence corresponding to characteristic signals of these molecules. Lobophorenol A was not detected by LC-MS while it was observed as marker in NMR because of some characteristic signals at δ_H 3.70 (H-4) and 6.02 ppm (H-2; see Fig. S1). The absence of detection of lobophorenol A by LC-MS might stem from a high reactivity of the chlorinated derivative during ionization. These lobophorenols have been shown to present allelopathic effects against the coral *Acropora muricata* (Vieira et al., 2016). Molecular networking based on MS^2 spectra analyses did not allow identification of additional chemomarkers. Annotation of compounds from marine organisms, especially macroalgae, is still challenging with the lack of specific databases. Altogether, LC-MS and NMR provide complementary approaches to analyze the metabolome and their combination is highly relevant to discriminate *Lobophora* species, as supported by the MFA.

NMR analyses also showed the rich composition in lipidic derivatives of *Lobophora* species, which may be problematic because intense long-fatty-chain signals may mask other signals. However, this issue could be resolved using GC-MS, allowing the study of the non-polar part of the metabolome. Compared to the poor specialized LC-MS database, the available GC-MS databases enabled the annotation of some chemomarkers. However, the discrimination between species metabotypes was partly explained by compounds presumably identified as pollutants from plastic origin and present in the coastal sites, which were likely differently accumulated in the algae or at their surface as seen in *Sargassum* spp. and *Fucus vesiculosus* (Chan et al., 2004; Gutow et al., 2016). This result potentially highlights more different adhesion capacities of microplastics between species rather than metabolic differences. Other markers evidenced by the NMR method include: 2-pentenoic, which is a small unsaturated fatty acid previously found in plants (Wu and Chen, 1992). Pentenoic acid was found up-regulated under salinity stress in the halophyte *Aeluropus lagopoides* (Paidi et al.,2017). Maleimide, 2-methyl-3-vinyl was also detected in the algal samples. This metabolite may be a transformation product of chlorophylls and bacteriochlorophylls (Naeher et al., 2013). We hypothesize that these compounds originate in part from micro-organisms associated to *Lobophora* species. Indeed, epiphytes often colonized the

algal surface (Egan et al., 2013). Then, by extracting the algal metabolome, we may also extract compounds from bacteria or epiphytes and metabotypes observed in our study may arise, at least in part, from the algal-associated organisms. Even if we carefully removed epiphytes from their surface, microorganisms are still present and may contribute to the global metabolome of the specimens. For example, methyl stearate has been found in bacteria and plants but also microalgae, ascidians and macroalgae (De Rosa et al., 2001; Sharmin et al., 2016; Takeara et al., 2008; Terekhova et al., 2010) and is assumed to have antibacterial and cytotoxic activities (Elshafie et al., 2017; Takeara et al., 2008). The influence of species-specific microbial communities, which can produce minor compounds, may also explained the better result obtain by LC-MS in the discrimination of *Lobophora* species.

Even if less important than interspecific differences, intraspecific variability can be explained by their development stage, life history traits and evolution and may also result from their environment. *Lobophora* life cycle is not documented in New Caledonia lagoon and reproductive state has been seen all year round (Vieira, personal observation). Gametophytes and sporophytes are not easily dissociable but may potentially present different chemical profiles as seen in other macroalgae, like the red algae *Portieria hornemannii* in the Philippines (Payo et al., 2011). The close association of *L. rosacea* and *L. monticola* with corals could lead to chemical adaptation or specification in the algal chemistry, notably against coral associated microbiome. On the other hand, growing in algal beds, *L. sonderii* is more exposed to herbivores and its chemistry probably evolved differently, notably to repulse predators. *Lobophora obscura* is also exposed to other organisms but its encrusting form with thick and coarse thalli, may deter predators. Less effort in metabolites production may be balanced by its protective morphology. Because very few chemomarkers were identified, these hypotheses should be further investigated and tested. Moreover, regarding the good discrimination observed with LC-MS in this work, this method may be useful to separate cryptic species of *Lobophora*, as successfully applied for *Portieria dioli* (Payo et al., 2011).

The choice of the technique to accurately distinguish species is pivotal and only few studies comparing these techniques have been published to date, most of them being applied to plants. For example, untargeted LC-MS was the most effective to discriminate several green tea (Kellogg et al., 2017). Other authors used multiple approaches to study the metabolomic fingerprint in zoanthids (Costa-Lotufo et al., 2018) or in the plant kingdom (Agnolet et al., 2010; Farag et al., 2012b). Multiple metabolomics approaches are rare on macroalgae. Notably, LC-MS and HR-MAS NMR were used to evaluate the relevance for taxonomical purpose in five species of the genus *Cystoseira* (Jégou et al., 2010). Due to the high diversity in metabolites, with diverse physico-chemical properties and different concentration ranges, the global analysis in metabolites is challenging. Using multiple metabolomics approaches allow a broader analysis. It is a good tool to appreciate the chemical diversity among species and can bring complementary information to the phylogenetic data, the unavoidable base for classification. These approaches enabled a better exploration of the chemical speciation or evolution among genus or even at a broader scale, as realized by Belghit et al.(2017) on 21 species belonging to red, green and brown algae. With the increase of shared metabolomics platforms, metabolomic fingerprinting might be applied to other macroalgae and marine organisms, and when coupled with genomics or transcriptomics, it will greatly improve our understanding of adaptive mechanisms involved in multi-stressors environments. This coupling has been recently applied to macroalgae, like in the model *Ectocarpus siliculosus* where transcriptomic and genomic data available allowed to better understand the metabolic changes during saline and oxidative stress (Dittami et

al., 2011) or under different CO_2 and O_2 concentrations (Gravot et al., 2010). While *Lobophora* genus is not a typical model organism, the decreased cost and increased sequencing capabilities of Next Generation Sequencing make it possible to examine species beyond traditional models (Konotchick et al., 2013; Unamba et al., 2015). In particular, it is an example of common brown alga widely distributed in tropical waters and producing major non-polar metabolites and therefore can represent a model for other metabolomic studies applied to brown algae. A coupling between metabolomics and meta-genomics could also help to understand the diversity of associated bacteria and better assess their contribution to the algal metabolome. Because associated microorganisms are commonly species-specific, this could partly explain the better results obtained with LC-MS. While a multiple metabolomic approach is promising for several applications in macroalgae, data interpretation remain the biggest challenge to date and more metabolomics studies on macroalgae are needed.

4. Conclusion

Metabolic fingerprinting with LC-MS was the most appropriate technique in the discrimination of different *Lobophora* species, but the coupling with NMR is also useful as the main metabolites can be observed with these methods and identified as chemomarkers. Indeed, lobophorenols, previously identified specialized metabolites in *L. rosacea,* were detected as chemomarkers with both LC-MS and NMR while they were not detected by GC-MS, which appeared a less useful technique for analyzing the *Lobophora* genus. This study demonstrates that an untargeted metabolomic approach via LC-MS/NMR will be helpful for further ecological studies in *Lobophora.* Notably, this technique is appropriate to explore the sources of metabolomic variations in this genus at the temporal and spatial scales, influenced by environmental factors, and also in response to different biotic interactions.

5.Experimental

5.1. Sampling

Lobophora rosacea, L. sonderii and *L. obscura* were collected by SCUBA during summer 2016 at Ricaudy (22°18.956'S; 166°27.405'E, Nouméa, New Caledonia). *Lobophora monticola* was collected during summer 2016 at Sainte-Marie (22°18.269'S; 166°28.791'E, Nouméa, New Caledonia). Species identifications were performed by combining morphological and genetic analyses following Vieira *et al.*(2014). Vouchers for each species are kept at IRD herbarium (IRD10213, IRD10195, IRD10187, IRD10199). *Lobophora rosacea* has a thin fan-shaped thallus, growing fixed by the basal part within coral branches like *Acropora* spp. *Lobophora monticola* is also found associated to branching corals, and thalli grows partially or completely in contact with them. *Lobophora sonderii* forms dense erected blades, mixed with other brown seaweeds in *Sargassum* beds. Conversely, *L. obscura* has encrusting and thick leather-like thalli, strongly attached to dead corals or coral rubbles (Fig. 5). Specimens (six for *L. rosacea, L. monticola* and *L. obscura* and five for *L. sonderii)* were placed in separate ziplock plastic bags, immediately placed into ice and stored at -20 °C until sample grinding.

5.2. Metabolite extractions

Algae were freeze-dried and manually ground with liquid nitrogen in a mortar. Samples were then stored in silicagel until chemical extractions. For each replicate, a mass of 250 mg was extracted 3 times with 5 mL of MeOH/CH_2Cl_2(1:1) during 5 min in an ultrasonic bath. Supernatants were pooled and filtered from samples. The extracts were concentrated to dryness in the presence of C18 silica powder (100 mg, Polygoprep 60-50, Macherey-Nagel®) using a rotary evaporator, and the solid was then fractioned by Solid Phase Extraction (SPE, Strata C18-E 500 mg/6 mL, Phenomenex®) by the successive elution of H_2O (6 mL), MeOH (6 mL) and CH_2Cl_2 (6 mL) after cartridge cleaning (6 mL MeOH/CH_2Cl_2) and conditioning (6 mL H_2O). The MeOH fractions were then filtered on syringe filters (PTFE, 0.20 µm, Phenomenex®), dried in a speedvac and further used for UHPLC-QToF and NMR analyses. The CH_2Cl_2fractions were only analyzed by GC/MS.

5.3. Metabolomic analyses

5.3.1. NMR

Dry samples were dissolved in 0.5 mL $CDCl_3$. ^{1}H-NMR spectra were recorded on a cryoprobe-equipped 600 MHz Agilent spectrometer. The following parameters were used for data acquisition: 16 ppm spectral width, 1 s relaxation delay with water pre-saturation (PS), number of scans 32, acquisition time 1.7 s, 16 K complex data points, 90° pulse angle.

5.3.2 UHPLC-QToF

Metabolomic fingerprints were recorded on an UHPLC (Dionex Ultimate 3000, Thermo Scientific®) coupled to an accurate mass spectrometer equipped with an ESI source (QqToF Impact II, Bruker Daltonics®). Metabolite separation were performed on a C18 UHPLC column (Acclaim™ RSLC 120 C18 150 x 2.1 mm, 2.2 µm, Thermo Scientific®) at 40 °C. The mobile phase consisted in a mix of H_2O + 0.1 % formic acid + 10 mM ammonium formate (solvent A) and acetonitrile/H_2O (95:5) + 0.1 % formic acid + 10 mM ammonium formate (solvent B). Injection volume was set to 3 µL and elution flow to 0.4 mL min^{-1}. The elution gradient was programmed as follows: 40 % B during 2 min, increased up to 100 % B from 2 to 8 min, followed by an isocratic step of 100% B during 4 min. The initial conditions were gradually recovered from 12 to 14 min, and hold 3 min for column equilibration for a total runtime of 17 min. MS parameters were set as follows: nebulizer gas N_2 at 40 psig, gas temperature 300 °C, drying gas N_2 flow 4 L min^{-1}, capillary voltage 3500 V. Mass spectra were acquired in positive ionization mode from 50 to 1,200 amu at 2 Hz. Auto-MS² spectra were acquired according to the same conditions then previously. A quality control sample (QC) was prepared with 25 µL of each sample. It was used to check MS shift over time and to normalize data according to injection order. The run started with three blank injections, followed by 10 injections of the QC for mass spectrometer stabilization. Samples were then randomly injected, inserting one QC every five samples. A final blank was injected to check any memory effect of the compounds on the column.

5.3.3 GC-MS

CH_2Cl_2 fractions were analyzed on a gas chromatograph (7890B GC System - 7693 autosampler, Agilent Technologies®) coupled to a mass selective detector (5977A MSD, Agilent Technologies®). Separation of metabolites was performed on a HP-5MS 5% Phenyl-Methyl Silox column (30 m x 0.25 mm, 0.25 µm, Agilent Technologies®) with helium as mobile phase. The run started at 40 °C for 5 min and increased by 10 °C min^{-1} up

to 300°C for a total runtime of 31 min. A constant flow rate was set to 1 mL min^{-1}. A volume of 1 µL of each sample was injected in splitless mode at 250°C. A solution with a mix of C8-C20 and C21-C40 alkanes (Fluka Analytical) was also injected for the determination of compound retention index.

5.3.4 Data treatment

^{1}H-NMR spectra were automatically Fourier-transformed and processed on MesReNova 11. Spectra baselines were automatically corrected followed by the Whittaker smoother correction. An equal width bucketing of 0.001 ppm was applied between 0-8 ppm to finally obtain the data matrix. Data were auto-scaled and log-transformed before statistical analyses.

LC–MS raw data files were first calibrated before converting them to netCDF files (centroid mode) using Bruker Compass DataAnalysis 4.3. NetCDF files were processed using the package XCMS for R software (version 3.3.2, XCMS version 1.50.1). Optimized parameters for XCMS were used as follows: peak picking (method= "centwave", peakwidth= c(2,20), ppm= 15, mzdiff= 0.05, prefilter= c(0,0)), retention time correction (method = "obiwarp"), matching peaks across samples (bw= 30, mzwid= 0.015, minfrac= 0.3) and filling in missing peaks. The matrix was then cleaned according to blanks and pooled samples to remove analytical variability. Molecular network based on MS^2 spectra were constructed with GNPS (Wang et al., 2016) and managed under Cytoscape 3.5.0 (Shannon et al., 2003).

Agilent data files acquired from GC-MS analysis were exported into CDF files using MSD Chemstation (F.01.001903, Agilent Technologies®). CDF files were then processed using the package eRah (version 1.0.5, Domingo-Almenara et al., 2016) under R performing preprocessing, peak deconvolution (min.peak.width = 2.5, min.peak.height=2500, noise.threshold=500, avoid.processing.mz=c(73,149,207)), peak alignment (min.spectra.cor=0.90, max.time.dist=60, mz.range=40:500) and missing compound recovery (with presence required in 3 samples at least). Compound annotation was performed manually by comparing mass spectra with NIST 2011 database completed with the calculation of Kovàts' index (Van Den Dool and Kratz, 1963). The matrix obtained was finally filtered according to the blank. Data from LC-MS and GC-MS were normalized by log-transformation before statistical analyses.

5.4. Statistical analyses

Principal component analysis (PCA) was used to visualize the metabolome variation according to species (ade4 package for R). Powered Partial Least-Squares-Discriminant Analysis (PPLS-DA) identified the maximum covariance between our data set and their class membership and permutational tests based on cross model validation (MVA.test and pairwise.MVA.test) were used to test differences between groups (RVAideMemoire package). Discriminating compounds were then identified according to the PPLS-DA loading plots (correlation circles; RVAideMemoire package). Multiple Factor Analysis (MFA, variables scaled to unit variance) was used to combine data obtained from LC-MS and NMR (FactoMineR and factoextrapackages for R). Kruskal-Wallis tests were performed in MetaboAnalyst 3.0 and R (PMCMR package). Post-hoc Conover's test was done on R software (PMCMR package). Venn diagram was constructed with Venny 2.1 (Oliveros 2007-2015).

Acknowledgments: GC-MS fingerprints were acquired at IMBE Support Service on Chemical Ecology and Metabolomics (funded by the CNRS, the Provence Alpes Côte d'Azur Region, the TOTAL Foundation and ANR). We are grateful to J-C. Martin for in-house R scripts. R. Doohan is acknowledged for her help in the NMR analyses and H. Solanki for his support in UHPLC-QToF analyses. We are grateful to C. Vieira, G. Culioli and M. Zubia for their useful comments. The PhD of J. Gaubert is supported through a scholarship from Sorbonne University, Paris, France.

Conflict of Interest: The authors declare no conflicts of interest.

References

Abdo, D.A., Motti, C.A., Battershill, C.N., Harvey, E.S., 2007. Temperature and spatiotemporal variability of salicylihalamide A in the sponge *Haliclona* sp. J. Chem. Ecol. 33, 1635–1645. https://doi.org/10.1007/s10886-007-9326-x

Agnolet, S., Jaroszewski, J.W., Verpoorte, R., Staerk, D., 2010. 1H NMR-based metabolomics combined with HPLC-PDA-MSSPE- NMR for investigation of standardized *Ginkgo biloba* preparations. Metabolomics 6, 292–302. https://doi.org/10.1007/s11306-009-0195-x

Belghit, I., Rasinger, J.D., Heesch, S., Biancarosa, I., Liland, N., Torstensen, B., Waagbø, R., Lock, E.J., Bruckner, C.G., 2017. In-depth metabolic profiling of marine macroalgae confirms strong biochemical differences between brown, red and green algae. Algal Res. 26, 240–249. https://doi.org/10.1016/j.algal.2017.08.001

Bundy, J.G., Davey, M.P., Viant, M.R., 2009. Environmental metabolomics: A critical review and future perspectives. Metabolomics 5, 3–21. https://doi.org/10.1007/s11306-008-0152-0

Bussell, J.A., Gidman, E.A., Causton, D.R., Gwynn-Jones, D., Malham, S.K., Jones, M.L.M., Reynolds, B., Seed, R., 2008. Changes in the immune response and metabolic fingerprint of the mussel, *Mytilus edulis* (Linnaeus) in response to lowered salinity and physical stress. J. Exp. Mar. Bio. Ecol. 358, 78–85. https://doi.org/10.1016/j.jembe.2008.01.018

Cachet, N., Genta-Jouve, G., Ivanisevic, J., Chevaldonné, P., Sinniger, F., Culioli, G., Pérez, T., Thomas, O.P., 2015. Metabolomic profiling reveals deep chemical divergence between two morphotypes of the zoanthid *Parazoanthus axinellae*. Sci. Rep. 5, 8282. https://doi.org/10.1038/srep08282

Campos De Paula, J., Bomeny Bueno, L., Christina De Palmer Paixao Frugulhetti, I., Yoneshigue-Valentin, Y., Laneuville Teixeira, V., 2007. *Dictyota dolabellana* sp. nov. (Dictyotaceae, Phaeophyceae) based on morphological and chemical data. Bot. Mar. 50, 288–293. https://doi.org/10.1515/BOT.2007.033

Cantillo-Ciau, Z., Moo-Puc, R., Quijano, L., Freile-Pelegrín, Y., 2010. The tropical brown alga *Lobophora variegata*: a source of antiprotozoal compounds. Mar. Drugs 8, 1292–304. https://doi.org/10.3390/md8041292

Chan, H.W., Lau, T.C., Ang, P.O., Wu, M., Wong, P.K., 2004. Biosorption of di (2-ethylhexyl) phthalate by seaweed biomass. J. Appl. Phycol. 263–274. https://doi.org/10.1023/B:JAPH.0000047778.93467.af

Connan, S., Goulard, F., Stiger, V., Deslandes, E., Gall, E.A., 2004. Interspecific and temporal variation in phlorotannin levels in an assemblage of brown algae. Bot. Mar. 47, 410–416. https://doi.org/10.1515/BOT.2004.057

Costa-Lotufo, L. V., Carnevale-Neto, F., Trindade-Silva, A.E., Silva, R.R., Silva, G.G.Z., Wilke, D. V., Pinto, F.C.L., Sahm, B.D.B., Jimenez, P.C., Mendonça, J.N., Lotufo, T.M.C., Pessoa, O.D.L., Lopes, N.P., 2018. Chemical profiling of two congeneric sea mat corals along the Brazilian coast: adaptive and functional patterns. Chem. Commun. https://doi.org/10.1039/C7CC08411K

De Rosa, S., Kamenarska, Z., Bankova, V., Stefanov, K., Dimitrova-Konaklieva, S., Najdenski, H., Tzevtkova, I., Popov, S., 2001. Chemical composition and biological activities of the Black Sea algae *Polysiphonia denudata* (Dillw.) Kutz. and *Polysiphonia denudata f. fragilis* (Sperk) woronich. Zeitschrift fur

Naturforsch. - Sect. C J. Biosci. 56, 1008–1014. https://doi.org/10.1515/znc-2001-11-1218

Dittami, S.M., Gravot, A., Renault, D., Goulitquer, S., Eggert, A., Bouchereau, A., Boyen, C., Tonon, T., 2011. Integrative analysis of metabolite and transcript abundance during the short-term response to saline and oxidative stress in the brown alga *Ectocarpus siliculosus*. Plant, Cell Environ. 34, 629–642. https://doi.org/10.1111/j.1365-3040.2010.02268.x

Domingo-Almenara, X., Brezmes, J., Vinaixa, M., Samino, S., Ramirez, N., Ramon-Krauel, M., Lerin, C., Díaz, M., Ibáñez, L., Correig, X., Perera-Lluna, A., Yanes, O., 2016. ERah: A Computational Tool Integrating Spectral Deconvolution and Alignment with Quantification and Identification of Metabolites in GC/MS-Based Metabolomics. Anal. Chem. 88, 9821–9829. https://doi.org/10.1021/acs.analchem.6b02927

Egan, S., Harder, T., Burke, C., Steinberg, P., Kjelleberg, S., Thomas, T., 2013. The seaweed holobiont: Understanding seaweed-bacteria interactions. FEMS Microbiol. Rev. 37, 462–476. https://doi.org/10.1111/1574-6976.12011

Elshafie, H.S., Racioppi, R., Bufo, S.A., Camele, I., 2017. In vitro study of biological activity of four strains of *Burkholderia gladioli* pv. *agaricicola* and identification of their bioactive metabolites using GC–MS. Saudi J. Biol. Sci. 24, 295–301. https://doi.org/10.1016/j.sjbs.2016.04.014

Farag, M.A., Porzel, A., Schmidt, J., Wessjohann, L.A., 2012a. Metabolite profiling and fingerprinting of commercial cultivars of *Humulus lupulus* L. (hop): A comparison of MS and NMR methods in metabolomics. Metabolomics 8, 492–507. https://doi.org/10.1007/s11306-011-0335-y

Farag, M.A., Porzel, A., Wessjohann, L.A., 2012b. Comparative metabolite profiling and fingerprinting of medicinal licorice roots using a multiplex approach of GC-MS, LC-MS and 1D NMR techniques. Phytochemistry 76, 60–72. https://doi.org/10.1016/j.phytochem.2011.12.010

Fiehn, O., 2002. Metabolomics - the link between genotyopes and phenotypes. Plant Mol. Biol. 48, 155–171.https://doi.org/10.1023/A:1013713905833

Gerwick, W., Fenical, W., 1982. Phenolic lipids from related marine algae of the order dictyotales. Phytochemistry 21, 633–637. https://doi.org/10.1016/0031-9422(82)83154-3

Gravot, A., Dittami, S.M., Rousvoal, S., Lugan, R., Eggert, A., Collén, J., Boyen, C., Bouchereau, A., Tonon, T., 2010. Diurnal oscillations of metabolite abundances and gene analysis provide new insights into central metabolic processes of the brown alga *Ectocarpus siliculosus*. New Phytol. 188, 98–110. https://doi.org/10.1111/j.1469-8137.2010.03400.x

Greff, S., Zubia, M., Payri, C., Thomas, O.P., Perez, T., 2017. Chemogeography of the red macroalgae *Asparagopsis*: metabolomics, bioactivity, and relation to invasiveness. Metabolomics 13, 0. https://doi.org/10.1007/s11306-017-1169-z

Gutiérrez-Cepeda, A., Fernández, J.J., Norte, M., Montalvão, S., Tammela, P., Souto, M.L., 2015. Acetate-Derived Metabolites from the Brown Alga *Lobophora variegata*. J. Nat. Prod. 78, 1716–1722. https://doi.org/10.1021/acs.jnatprod.5b00415

Gutow, L., Eckerlebe, A., Giménez, L., Saborowski, R., 2016. Experimental Evaluation of Seaweeds as a Vector for Microplastics into Marine Food Webs. Environ. Sci. Technol. 50, 915–923. https://doi.org/10.1021/acs.est.5b02431

Ivanišević, J., Thomas, O.P., Lejeusne, C., Chevaldonné, P., Pérez, T., 2011a. Metabolic fingerprinting as an indicator of biodiversity: Towards understanding inter-specific relationships among Homoscleromorpha sponges. Metabolomics 7, 289–304. https://doi.org/10.1007/s11306-010-0239-2

Ivanišević, J., Thomas, O.P., Pedel, L., P??nez, N., Ereskovsky, A. V., Culioli, G., Pérez, T., 2011b. Biochemical trade-offs: Evidence for ecologically linked secondary metabolism of the sponge *Oscarella balibaloi*. PLoS One 6. https://doi.org/10.1371/journal.pone.0028059

Jaramillo, K.B., Reverter, M., Guillen, P.O., McCormack, G., Rodriguez, J., Sinniger, F., Thomas, O.P., 2018. Assessing the Zoantharian Diversity of the Tropical Eastern Pacific through an Integrative Approach. Sci. Rep. 8, 1–15. https://doi.org/10.1038/s41598-018-25086-4

Jégou, C., Culioli, G., Kervarec, N., Simon, G., Stiger-Pouvreau, V., 2010. LC/ESI-MSn and 1H HR-MAS NMR analytical methods as useful taxonomical tools within the genus *Cystoseira* C. Agardh (Fucales;

436 Phaeophyceae). Talanta 83, 613–622. https://doi.org/10.1016/j.talanta.2010.10.003

437 Kellogg, J.J., Graf, T.N., Paine, M.F., McCune, J.S., Kvalheim, O.M., Oberlies, N.H., Cech, N.B., 2017.
438 Comparison of Metabolomics Approaches for Evaluating the Variability of Complex Botanical
439 Preparations: Green Tea (*Camellia sinensis*) as a Case Study. J. Nat. Prod. 80, 1457–1466.
440 https://doi.org/10.1021/acs.jnatprod.6b01156

441 Konotchick, T., Dupont, C.L., Valas, R.E., Badger, J.H., Allen, A.E., 2013. Transcriptomic analysis of metabolic
442 function in the giant kelp, *Macrocystis pyrifera*, across depth and season. New Phytol. 198, 398–407.
443 https://doi.org/Doi 10.1111/Nph.12160

444 Kubanek, J., Jensen, P.R., Keifer, P. a, Sullards, M.C., Collins, D.O., Fenical, W., 2003. Seaweed resistance to
445 microbial attack: a targeted chemical defense against marine fungi. Proc. Natl. Acad. Sci. U. S. A. 100,
446 6916–21. https://doi.org/10.1073/pnas.1131855100

447 López-Legentil, S., Bontemps-Subielos, N., Turon, X., Banaigs, B., 2006. Temporal variation in the production
448 of four secondary metabolites in a colonial ascidian. J. Chem. Ecol. 32, 2079–2084.
449 https://doi.org/10.1007/s10886-006-9148-2

450 Mooney, B.D., Nichols, P.D., De Salas, M.F., Hallegraeff, G.M., 2007. Lipid, fatty acid, and sterol composition
451 of eight species of Kareniaceae (dinophyta): Chemotaxonomy and putative lipid phycotoxins. J. Phycol.
452 43, 101–111. https://doi.org/10.1111/j.1529-8817.2006.00312.x

453 Naeher, S., Schaeffer, P., Adam, P., Schubert, C.J., 2013. Maleimides in recent sediments - Using chlorophyll
454 degradation products for palaeoenvironmental reconstructions. Geochim. Cosmochim. Acta 119, 248–263.
455 https://doi.org/10.1016/j.gca.2013.06.004

456 Paidi, M.K., Agarwal, P., More, P., Agarwal, P.K., 2017. Chemical Derivatization of Metabolite Mass Profiling
457 of the Recretohalophyte *Aeluropus lagopoides* Revealing Salt Stress Tolerance Mechanism. Mar.
458 Biotechnol. 19, 207–218. https://doi.org/10.1007/s10126-017-9745-9

459 Payo, D.A., Colo, J., Calumpong, H., de Clerck, O., 2011. Variability of non-polar secondary metabolites in the
460 red alga *Portieria*., Marine drugs. https://doi.org/10.3390/md9112438

461 Pérez, T., Ivanisevic, J., Dubois, M., Pedel, L., Thomas, O.P., Tokina, D., Ereskovsky, A. V., 2011. *Oscarella*
462 *balibaloi*, a new sponge species (Homoscleromorpha: Plakinidae) from the Western Mediterranean Sea:
463 Cytological description, reproductive cycle and ecology. Mar. Ecol. 32, 174–187.
464 https://doi.org/10.1111/j.1439-0485.2011.00435.x

465 Rasher, D.B., Hay, M.E., 2010. Chemically rich seaweeds poison corals when not controlled by herbivores.
466 Proc. Natl. Acad. Sci. U. S. A. 107, 9683–8. https://doi.org/10.1073/pnas.0912095107

467 Rempt, M., Weinberger, F., Grosser, K., Pohnert, G., 2012. Conserved and species-specific oxylipin pathways in
468 the wound-activated chemical defense of the noninvasive red alga *Gracilaria chilensis* and the invasive
469 *Gracilaria vermiculophylla*. Beilstein J. Org. Chem. 8, 283–289. https://doi.org/10.3762/bjoc.8.30

470 Ritter, A., Dittami, S.M., Goulitquer, S., Correa, J. a, Boyen, C., Potin, P., Tonon, T., 2014. Transcriptomic and
471 metabolomic analysis of copper stress acclimation in *Ectocarpus siliculosus* highlights signaling and
472 tolerance mechanisms in brown algae. BMC Plant Biol. 14, 116. https://doi.org/10.1186/1471-2229-14-
473 116

474 Robinette, S.L., Bruschweiller, R., Schroeder, F., Edison, A.S., 2011. NMR in Metabolomics and Natural
475 Products Research: Two Sides of the Same Coin. Acc. Chem. Res. 45, 288–
476 297.https://doi.org/10.1021/ar2001606

477 Roessner, U., Bowne, J., 2009. What is metabolomics all about? Biotechniques 46, 363–365.
478 https://doi.org/10.2144/000113133

479 Rohde, S., Gochfeld, D.J., Ankisetty, S., Avula, B., Schupp, P.J., Slattery, M., 2012. Spatial Variability in
480 Secondary Metabolites of the Indo-Pacific Sponge *Stylissa massa*. J. Chem. Ecol. 38, 463–475.
481 https://doi.org/10.1007/s10886-012-0124-8

482 Shannon, P., Markiel, A., Owen Ozier, 2, Baliga, N.S., Wang, J.T., Ramage, D., Amin, N., Schwikowski, B.,
483 Ideker, T., 2003. Cytoscape: a software environment for integrated models of biomolecular interaction
484 networks. Genome Res. 13, 2498–2504. https://doi.org/10.1101/gr.1239303.metabolite

Sharmin, T., Monirul Hasan, C.M., Aftabuddin, S., Rahman, M.A., Khan, M., 2016. Growth, fatty acid, and lipid composition of marine microalgae *skeletonema costatum* available in Bangladesh coast: Consideration as biodiesel feedstock. J. Mar. Biol. 2016. https://doi.org/10.1155/2016/6832847

Slattery, M., Starmer, J., Paul, V.J., 2001. Temporal and spatial variation in defensive metabolites of the tropical Pacific soft corals *Sinularia maxima* and *S. polydactyla*. Mar. Biol. 138, 1183–1193. https://doi.org/10.1007/s002270100540

Takeara, R., Jimenez, P.C., Wilke, D.V., Odorico de Moraes, M., Pessoa, C., Peporine Lopes, N., Lopes, J.L.C., Monteiro da Cruz Lotufo, T., Costa-Lotufo, L.V., 2008. Antileukemic effects of *Didemnum psammatodes* (Tunicata: Ascidiacea) constituents. Comp. Biochem. Physiol. - A Mol. Integr. Physiol. 151, 363–369. https://doi.org/10.1016/j.cbpa.2007.02.011

Terekhova, E.A., Stepicheva, N.A., Pshenichnikova, A.B., Shvets, V.I., 2010. Stearic acid methyl ester: A new extracellular metabolite of the obligate methylotrophic bacterium *Methylophilus quaylei*. Appl. Biochem. Microbiol. 46, 166–172. https://doi.org/10.1134/S0003683810020079

Unamba, C.I.N., Nag, A., Sharma, R.K., 2015. Next Generation Sequencing Technologies: The Doorway to the Unexplored Genomics of Non-Model Plants. Front. Plant Sci. 6. https://doi.org/10.3389/fpls.2015.01074

Van Den Dool, H., Kratz, P., 1963. A generalization of the retention index system including linear temperature programmed gas—liquid partition chromatography. J. Chromatogr. A 11, 463–471. https://doi.org/10.1016/S0021-9673(01)80947-X

Vieira, C., Camacho, O., Sun, Z., Fredericq, S., Leliaert, F., Payri, C., De Clerck, O., 2017. Historical biogeography of the highly diverse brown seaweed *Lobophora* (Dictyotales, Phaeophyceae). Mol. Phylogenet. Evol. 110, 81–92. https://doi.org/10.1016/j.ympev.2017.03.007

Vieira, C., D'hondt, S., De Clerck, O., Payri, C.E., 2014. Toward an inordinate fondness for stars, beetles and *Lobophora*? Species diversity of the genus *Lobophora* (Dictyotales, Phaeophyceae) in New Caledonia. J. Phycol. 50, 1101–1119. https://doi.org/10.1111/jpy.12243

Vieira, C., Thomas, O.P., Culioli, G., Genta-Jouve, G., Houlbreque, F., Gaubert, J., De Clerck, O., Payri, C.E., 2016. Allelopathic interactions between the brown algal genus *Lobophora* (Dictyotales, Phaeophyceae) and scleractinian corals. Sci. Rep. 6, 18637. https://doi.org/10.1038/srep18637

Wang, M., Carver, J.J., Phelan, V. V., Sanchez, L.M., Garg, N., Peng, Y., Nguyen, D.D., Watrous, J., Kapono, C.A., Luzzatto-Knaan, T., 2016. Sharing and community curation of mass spectrometry data with Global Natural Products Social Molecular Networking. Nat. Biotechnol. 34, 828–837. https://doi.org/10.1038/nbt.3597

Wang, Y., Liu, S., Hu, Y., Li, P., Wan, J.-B., 2015. Current state of the art of mass spectrometry-based metabolomics studies – a review focusing on wide coverage, high throughput and easy identification. RSC Adv. 5, 78728–78737. https://doi.org/10.1039/C5RA14058G

Wink, M., 2003. Evolution of secondary metabolites from an ecological and molecular phylogenetic perspective. Phytochemistry 64, 3–19. https://doi.org/10.1016/S0031-9422(03)00300-5

Wu, C.M., Chen, S.Y., 1992. Volatile compounds in oils after deep frying or stir frying and subsequent storage. J. Am. Oil Chem. Soc. 69, 858–865. https://doi.org/10.1007/BF02636333

Figure and Table captions

Fig. 1. Discriminant power of the three chemical approaches via unsupervised (Principal Component Analysis, PCA, a, c, e) and supervised discriminant (Powered Partial Least-Squares-Discriminant Analysis, PPLS-DA, b, d, f) analyses of *Lobophora* species metabolome analyzed by (a, b) NMR for MeOH fractions and (c, d) LC-MS for MeOH fractions and (e, f) GC-MS for CH_2Cl_2 fractions (LO: *L. obscura* in red, LR: *L. rosacea* in orange,

LM: *L. monticola* in green and LS: *L. sonderii* in blue). CER = classification error rate with p-value after double cross model validation.

Fig. 2. Overlay of ^{1}H-NMR (600 MHz) spectra of the four *Lobophora* species (one representative sample per species was chosen, the full overlay spectra is available in Fig. S3. *L. monticola* in red, *L. obscura* in green, *L. rosacea* in blue and *L. sonderii* in purple). Regions of discriminating signals are highlighted by black rectangles.

Fig. 3. Box plots of lobophorenols B and C (and chemical structure of lobophorenols A-C) among the four *Lobophora* species and blank (log-transformed data, y-axis), detected by LC-MS, expressed as mean normalized intensities ± SD (n = 3 for blank, n = 6 for LM, LO, LR and n = 5 for LS)(LM: *L. monticola* in green, LO: *L. obscura* in red, LR: *L. rosacea* in orange and LS: *L. sonderii* in blue, x-axis). The statistical analyses were performed using Kruskal-Wallis (KW) followed by post-hoc Conover's test. Letters indicate significant differences between groups based on post-hoc pairwise comparisons ($p < 0.05$).

Fig. 4. Multiple Factor Analysis (MFA) obtained with LC-MS and NMR data from the MeOH fractions of *Lobophora* species (LM: *L. monticola* in green, LO: *L. obscura* in red, LR: *L. rosacea* in orange, and LS: *L. sonderii* in blue). Confidence level used to construct the ellipses = 0.95, variables scaled to unit variance.

Fig. 5. Pictures of *Lobophora* species: (a) *L. rosacea*, (b) *L. sonderii*, (c) *L. obscura* and (d) *L. monticola*. Arrows indicate algal thalli (algae were collected at Ricaudy for (a), (b), (c) and Sainte-Marie for (d); images by G. Boussarie).

Table 1. Chemomarkers detected by GC-MS in the CH_2Cl_2 fraction of *Lobophora* species, annotated with NIST 2011 database (COMP. = compound, RI = Van Den Dool and Kratz Retention Index, EXP. = experimental, LIT. = literature).

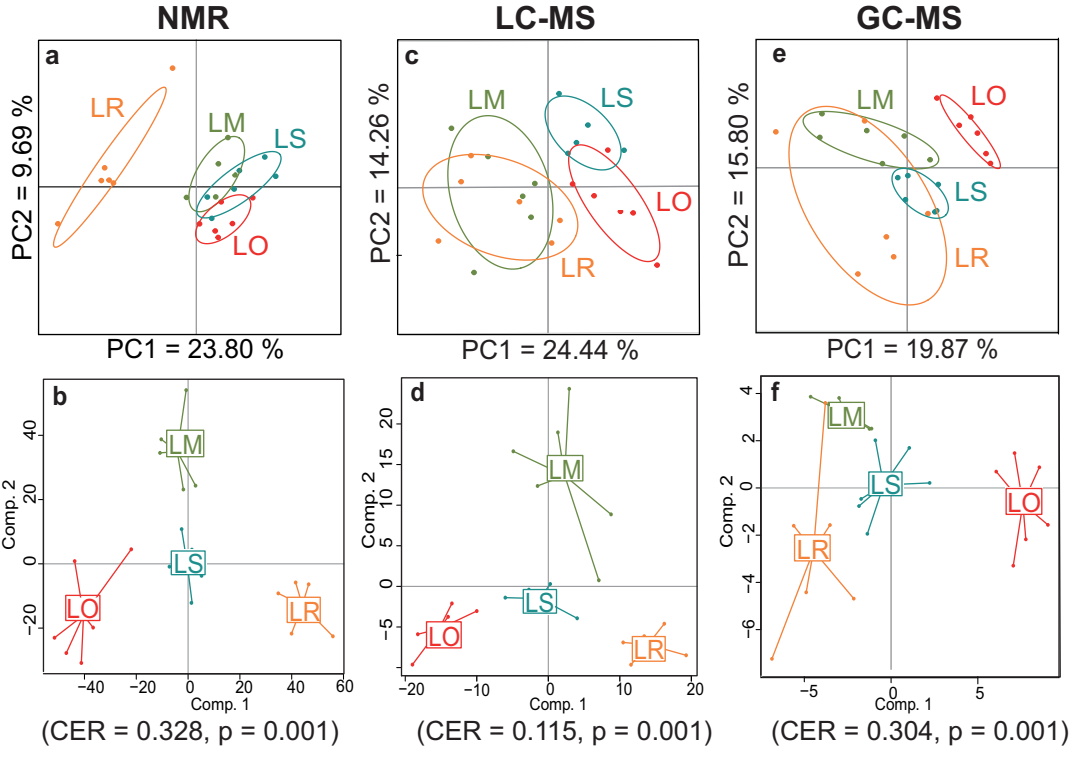
NMR
LC-MS
GC-MS
a
c
e
LR
LM
LS
LO
PC2 = 9.69 %
PC2 = 14.26 %
PC2 = 15.80 %
PC1 = 23.80 %
PC1 = 24.44 %
PC1 = 19.87 %
b
d
f
Comp. 1
Comp. 2
(CER = 0.328, p = 0.001)
(CER = 0.115, p = 0.001)
(CER = 0.304, p = 0.001)

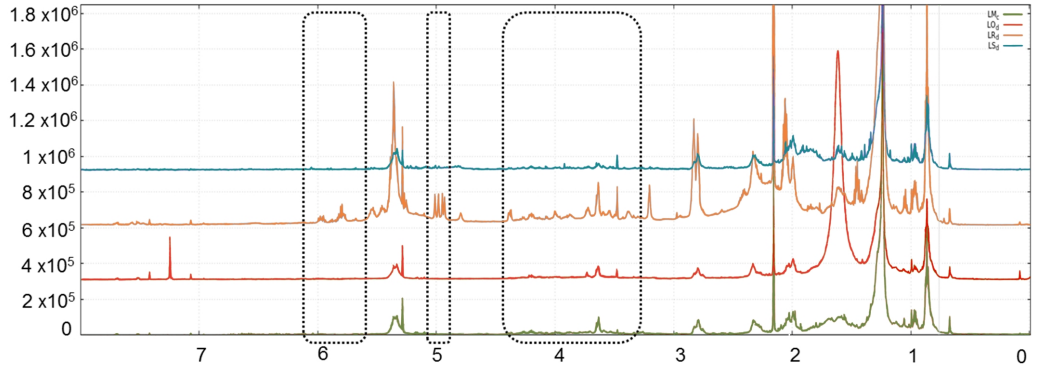
1.8 x10^6
1.6 x10^6
1.4 x10^6
1.2 x10^6
1 x10^6
8 x10^5
6 x10^5
4 x10^5
2 x10^5
0
7
6
5
4
3
2
1
0

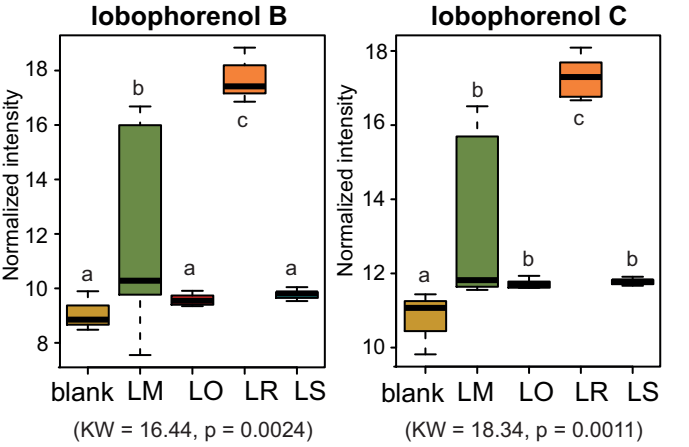
lobophorenol B
Normalized intensity
18
16
14
12
10
8
a
b
a
c
a
blank
LM
LO
LR
LS
(KW = 16.44, p = 0.0024)
lobophorenol C
Normalized intensity
18
16
14
12
10
a
b
b
c
b
blank
LM
LO
LR
LS
(KW = 18.34, p = 0.0011)

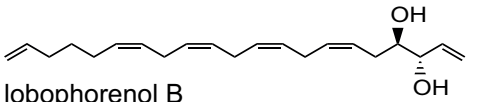
OH
OH
lobophorenol B

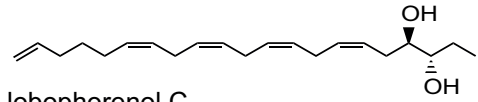
OH
OH
lobophorenol C

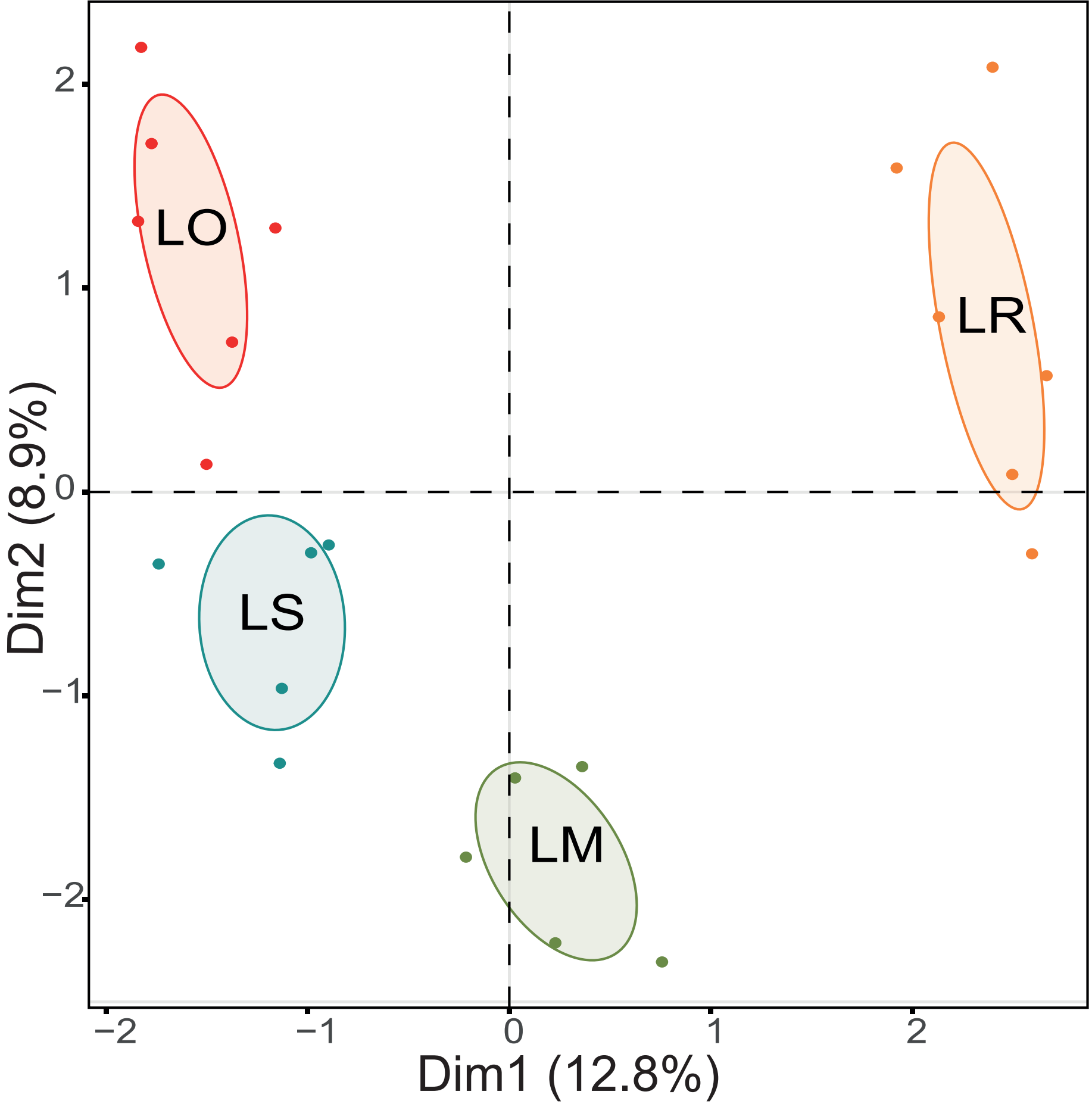
LO
LR
LS
LM
2
1
0
−1
−2
−2
−1
0
1
2
Dim2 (8.9%)
Dim1 (12.8%)

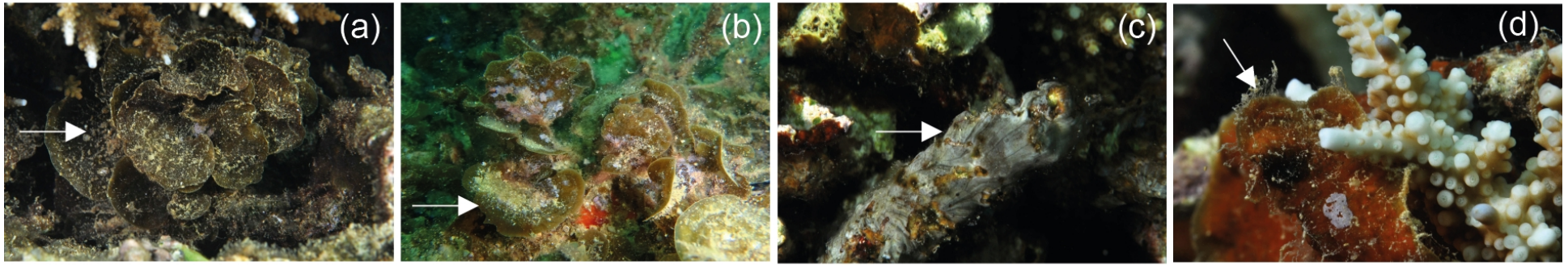
(a)
(b)
(c)
(d)

Table 1. Chemomarkers detected by GC-MS in the CH_2Cl_2 fraction of *Lobophora* species, annotated with NIST 2011 database (COMP. = compound, RI = Van Den Dool and Kratz Retention Index, EXP. = experimental, LIT. = literature).

COMP.	MOLECULAR NAME	CHEMICAL FAMILY	CAS NUMBER	RAW FORMULA	% MATCH NIST 2011	LIT. RI	EXP. RI
M5	2-pentenoic acid	carboxylic acid	626-98-2	$C_5H_8O_2$	94	873	921
M18	maleimide, 2-methyl-3-vinyl	amide	21494-57-5	$C_7H_7NO_2$	91	1261	1262
M38	methyl stearate	ester	112-61-8	$C_{19}H_{38}O_2$	98	2130	2129
M48	hexanoic acid, 2-ethyl-, hexadecyl ester	ester	59130-69-7	$C_{24}H_{48}O_2$	64	-	2468

SUPPLEMENTARY INFORMATION

Metabolomic variability of four macroalgal species of the genus *Lobophora* using diverse approaches

Julie GAUBERT[1,2], Stéphane GREFF[3], Olivier P. THOMAS[4]*, Claude E. PAYRI[2]*

[1] Sorbonne Universités, Collège Doctoral, F-75005 Paris, France.

[2] UMR ENTROPIE (IRD, UR, CNRS), Institut de Recherche pour le Développement, B.P. A5, 98848 Nouméa Cedex, Nouvelle-Calédonie, France.

[3] Institut Méditerranéen de Biodiversité et d'Ecologie Marine et Continentale (IMBE), UMR 7263 CNRS, IRD, Aix Marseille Université, Avignon Université, Station Marine d'Endoume, rue de la Batterie des Lions, 13007 Marseille, France.

[4] Marine Biodiscovery, School of Chemistry and Ryan Institute, National University of Ireland Galway (NUI Galway), University Road, H91 TK33 Galway, Ireland.

***corresponding authors**

Claude E. PAYRI: Tel 00687260750, claude.payri@ird.fr

Olivier P. THOMAS: Tel 0035391493563, olivier.thomas@nuigalway.ie

FIGURES

TABLES

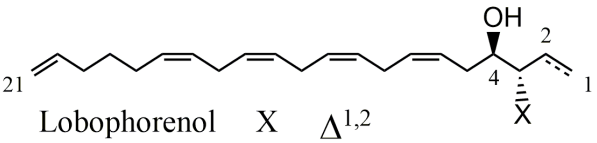

Lobophorenol	X	$\Delta^{1,2}$
A	Cl	yes
B	OH	yes
C	OH	no

Fig. S1. Chemical structure of lobophorenols A-C.

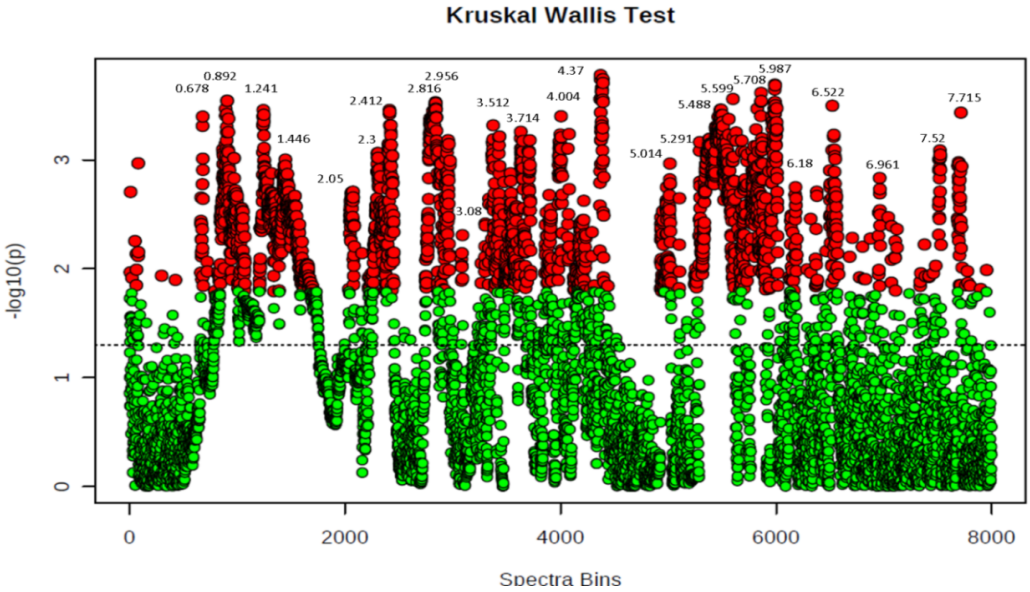

Fig. S2. Kruskal-Wallis test loading plots with bins varying among species in red ($p < 0.05$). Data were obtained with NMR.

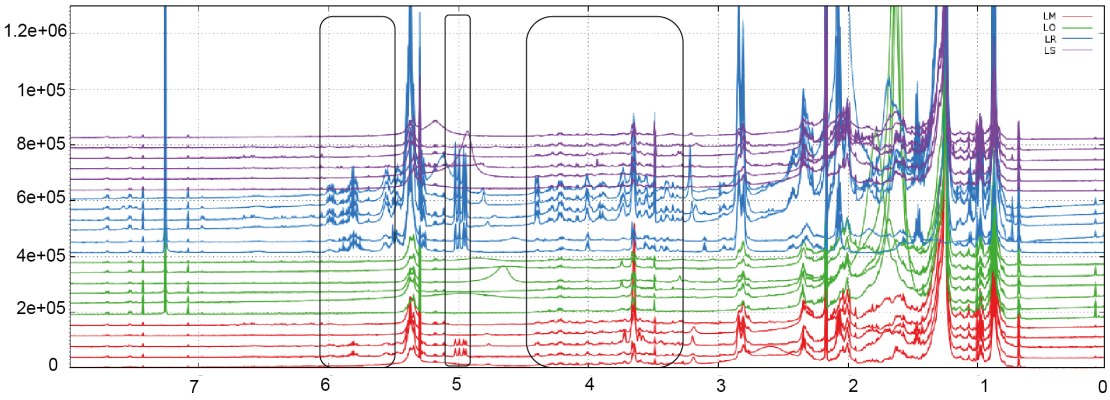

Fig. S3. Overlay of ^{1}H-NMR (600 MHz) spectra of the four *Lobophora* species (*L. monticola* in red, *L. obscura* in green, *L. rosacea* in blue and *L. sonderii* in purple). Regions of discriminating signals are highlighted by black rectangles.

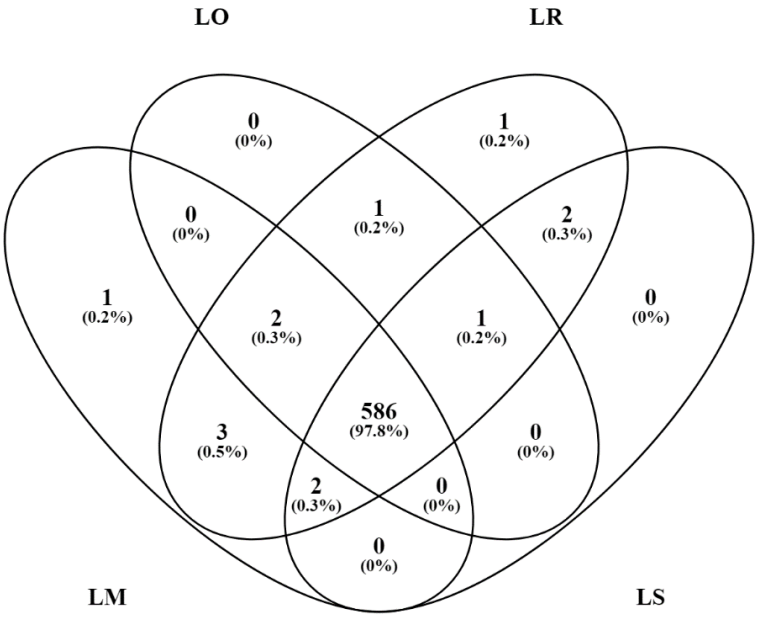

Fig. S4. Venn diagram test on *Lobophora* MeOH fractions analyzed by LC-MS (LO: *L. obscura*, LR: *L. rosacea*, LM: *L. monticola* and LS: *L. sonderii*). Minimal threshold was selected for each species when the ion intensity detected by LC-MS becomes very low and closed to the noise.

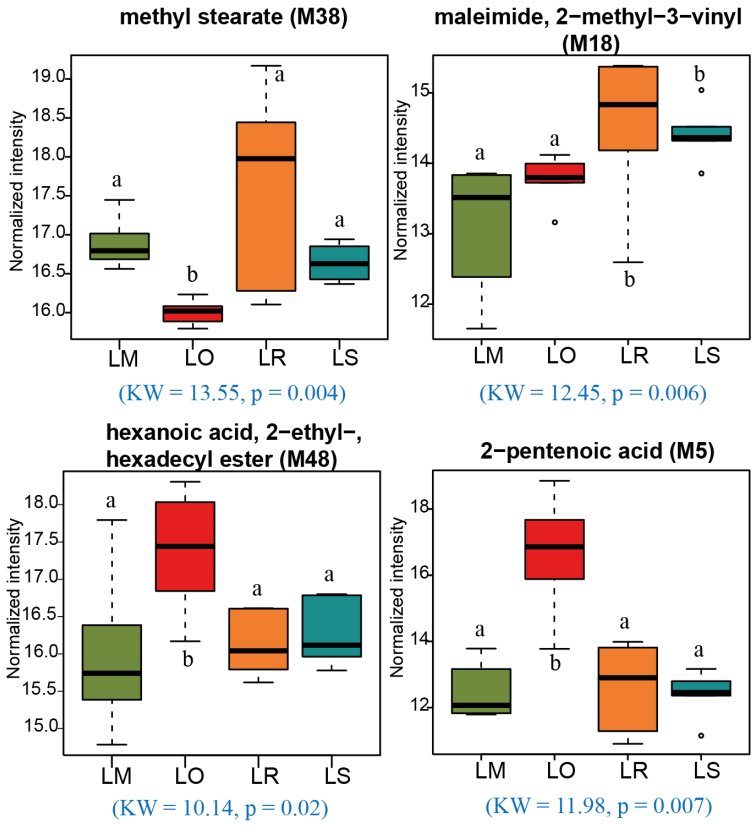

Fig. S5. Box plots of the chemomarkers annotated with NIST 2011 among the four *Lobophora* species (log-transformed data), detected by GC-MS, expressed as mean normalized intensities ± SD (n= 6 for each species) (LM: *L. monticola* in green, LO: *L. obscura* in red, LR: *L. rosacea* in orange, and LS: *L. sonderii* in blue). The statistical analyses were performed using Kruskal-Wallis (KW) followed by post-hoc Conover's test. Letters indicate distinct groupings based on post-hoc pairwise comparisons among groups for each compound ($p < 0.05$)

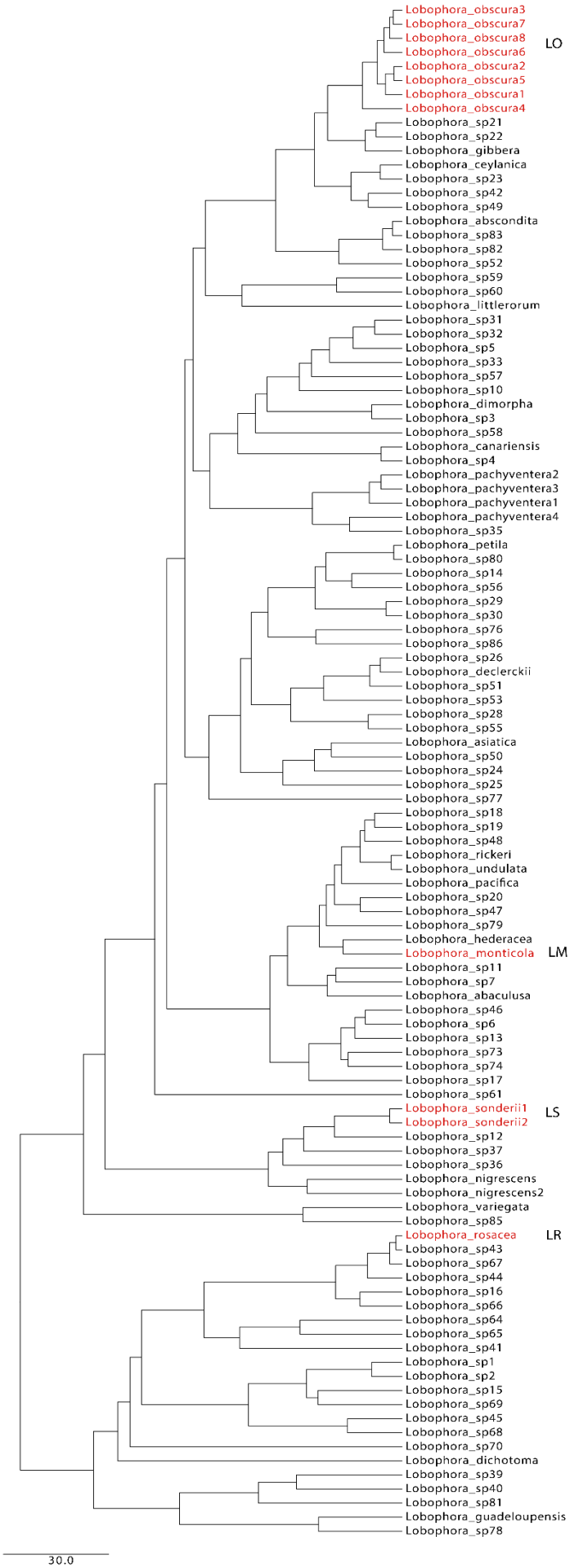

Fig. S6. *Lobophora* species tree reconstructed with BEAST using the mitochondrial marker cox3 and the chloroplast markers psbA and rbcL (adapted from Vieira et al. 2016, 2017) (LO: *L. obscura*, LR: *L. rosacea*, LM: *L. monticola* and LS: *L. sonderii*)

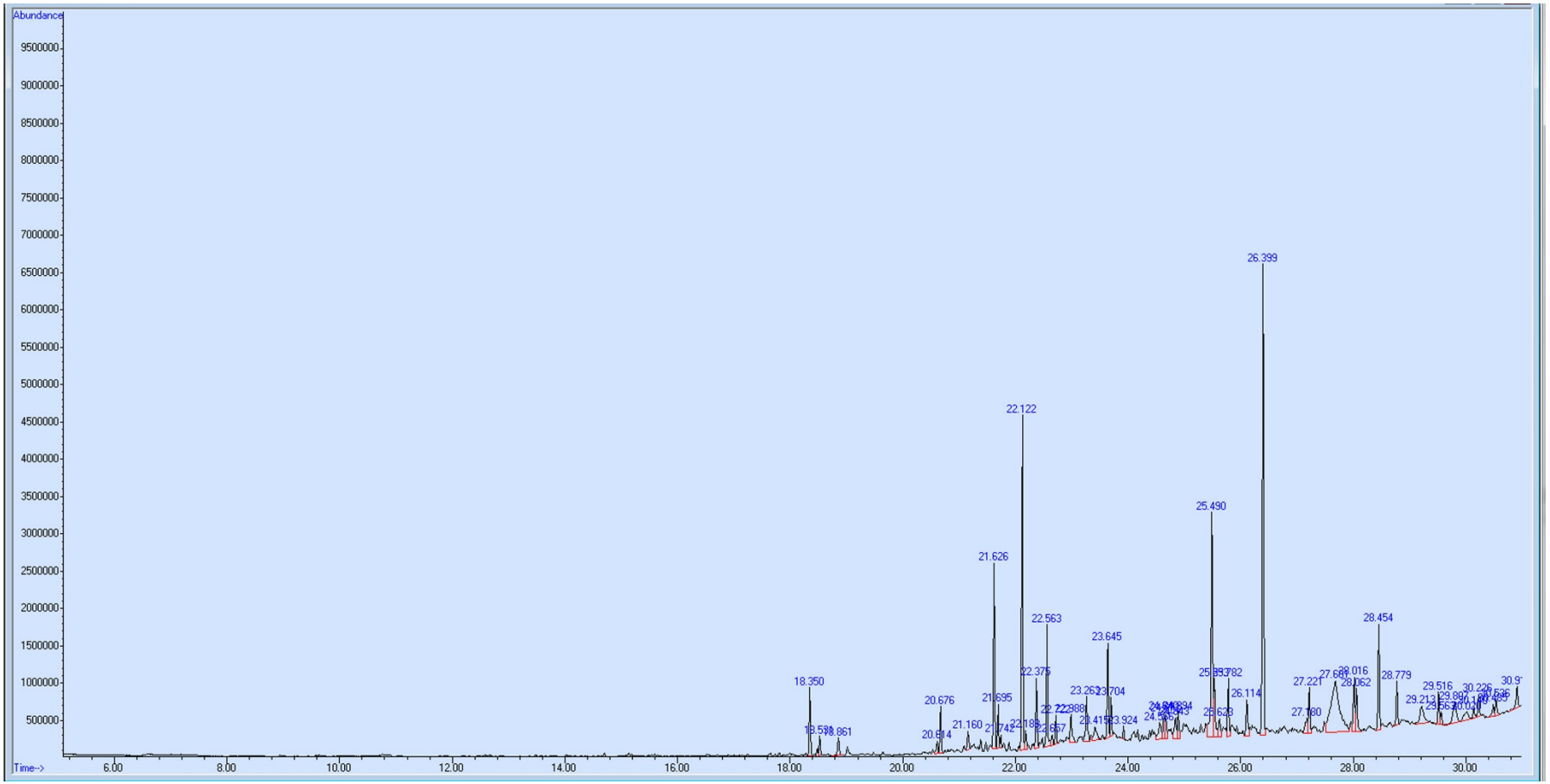

Fig. S7. Example of chromatogram obtained by GC-MS on the CH_2Cl_2 fraction of *Lobophora rosacea.*

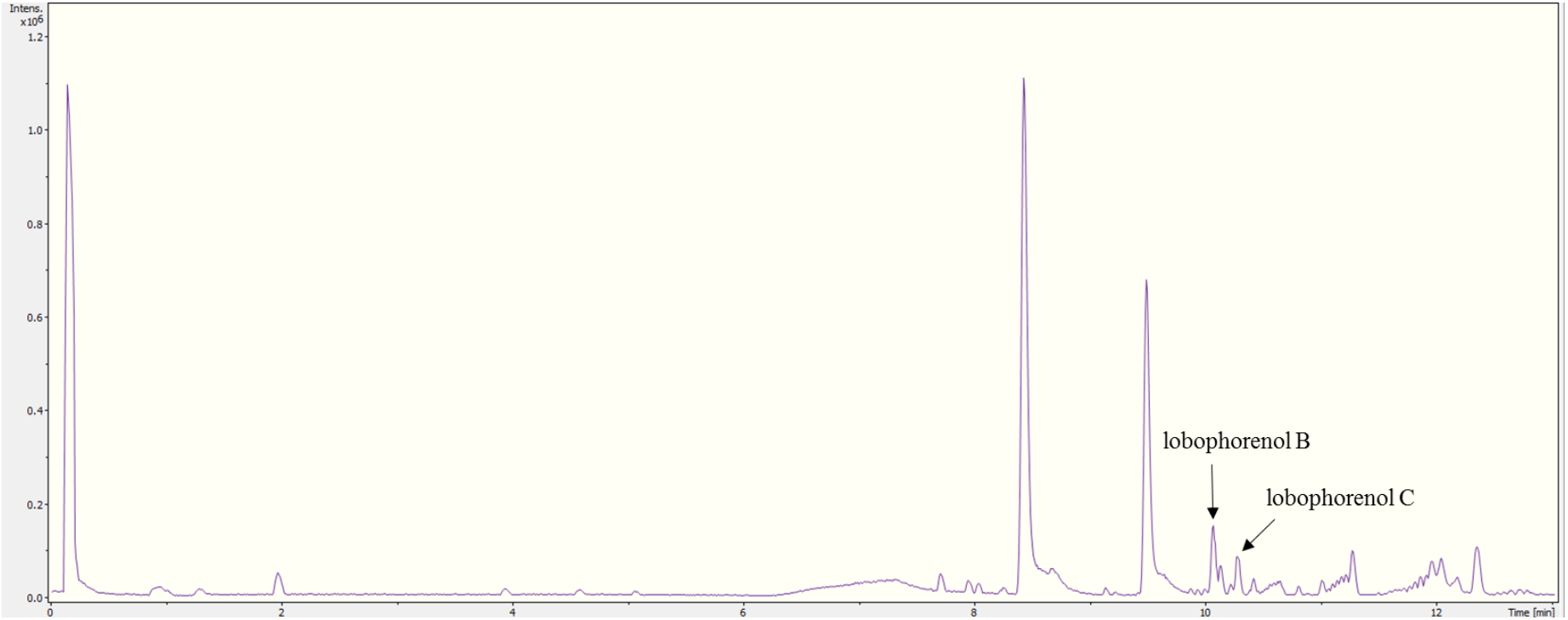

Fig. S8. Example of chromatogram obtained by LC-MS on the MeOH fraction of *Lobophora rosacea* with the elution peaks corresponding to the lobophorenols B and C.

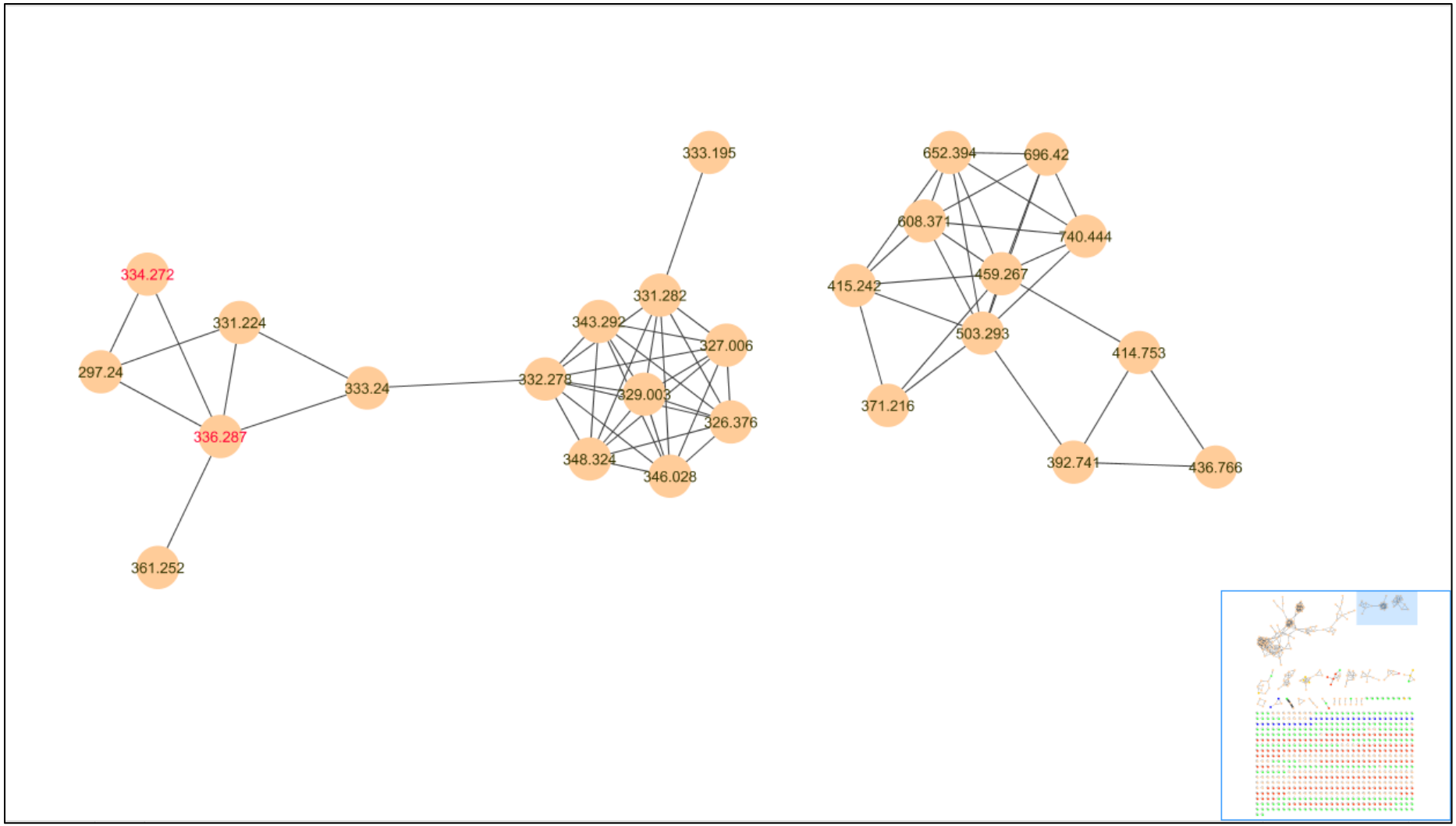

Fig. S9. Molecular network on MS² spectra managed under Cytoscape 3.5.0, with parent mass label. Lobophorenol B (m/z 334.272) and lobophorenols C (m/z 336.287) are in red.

Table S1. Post-hoc permutational pairwise test based on crossed model validation for metabotype differentiation according to species by NMR, LC-MS or GC-MS (999 permutations, p-value adjustment method: fdr). Significant p-values ($p < 0.05$) are in bold.

NMR				LC-MS				GC-MS			
	LM	LO	LR		LM	LO	LR		LM	LO	LR
LO	**0.018**	-	-	LO	**0.006**	-	-	LO	**0.006**	-	-
LR	**0.022**	**0.006**	-	LR	**0.044**	**0.006**	-	LR	0.431	**0.008**	-
LS	0.276	0.276	**0.018**	LS	**0.006**	**0.018**	**0.006**	LS	**0.012**	**0.008**	**0.018**

Table S2. Selection of the most significant regions in the spectra varying among *Lobophora* species (from Kruskal-Wallis test, with p-value < 0.05). Characteristic signals (ppm) of lobophorenols A, B and C are also assigned to the corresponding chemical shift range.

Max ppm area	**Range ppm area**	**Characteristic signals (ppm)**
0.678	0.662 - 0.68	-
0.892	0.823 - 0.997	Lobophorenol C: 0.97
1.214	1.237 - 1.253	-
1.446	1.407 -1.501	Lobophorenol C: 1.47 Lobophorenol A, B & C: 1.46
2.05	2.035 - 2.077	Lobophorenol B: 2.06, A & C: 2.07
2.3	2.08 - 2.386	Lobophorenol A: 2.10/2.25, B: 2.14, C: 2.24
2.412	2.318 - 2.433	Lobophorenol B & C: 2.36
2.816	2.747 - 2.836	Lobophorenol A, B & C: 2.82
2.956	2.85 - 3.08	Lobophorenol A: 2.86/2.87
3.374	3.240 - 3.442	Lobophorenol C: 3.32
3.512	3.365 - 3.595	Lobophorenol B: 3.48, C : 3.46
3.714	3.536 - 3.721	Lobophorenol A: 3.70
4.004	3.854 - 4.302	Lobophorenol B: 3.94
4.37	4.103 - 4.398	Lobophorenol A: 4.38
5.014	4.927 - 5.102	Lobophorenol A, B & C: 4.94 and 5.00
5.291	5.244 - 5.397	Lobophorenol A: 5.34, A, B & C: 5.37 and 5.38
5.488	5.398 - 5.667	Lobophorenol A: 5.48/5.49, B & C: 5.45 and Lobophorenol B: 5.51, C: 5.52
5.599	5.399 - 5.74	-
5.708	5.589 - 5.860	Lobophorenol B & C: 5.82
5.987	5.837 - 6.013	Lobophorenol B: 5.92
6.18	6.009 - 6.377	Lobophorenol A: 6.02
6.522	6.365 - 6.534	-
6.961	6.682 - 7.12	-
7.52	7.376 - 7.529	-
7.715	7.684 - 7.779	-

Table S3. *Lobophora* ions responsible for the difference according to species after LC-MS analysis. The mSigma (mS) value is a measure for the goodness of fit between experimental mass and isotopic pattern with theoretical ones: lower is the mS, better is the annotation.

m/z	rt	Ion assignation	Ion formula	error (ppm)	mS
334.2741	606	$[M + NH_4^+]$	$C_{21}H_{36}NO_2$	-2.5	9.4
336.2898	619	$[M + NH_4^+]$	$C_{21}H_{38}NO_2$	-1.5	21.5